



Cite this: *Org. Biomol. Chem.*, 2025, **23**, 2153

## Monoterpenoid selenophenes derived from (–)-carvone with GPx-like activity†

João P. Telo, \*<sup>a</sup> Luis F. Veiros, <sup>a</sup> Vânia André, <sup>a,b</sup> João Ferreira da Silva,<sup>a</sup> Gonçalo C. Justino <sup>‡a</sup> and Alexandra M. M. Antunes <sup>a</sup>

Organoselenium compounds have been recognized as potential therapeutic agents against several diseases. Specifically, the incorporation of selenium into natural products has been reported to produce positive synergistic biological effects. We report herein the one-pot reaction of the natural monoterpene (–)-carvone with selenium bromide, which yields mentoselenophenone **1**, together with minor amounts of phenols **2** and **3**. A number of derivatives of **1** have also been prepared: the  $\alpha,\alpha$  dimer **6**, oxime **7** and its Beckmann rearrangement product lactam **8**. All except lactam **8** showed antioxidant GPx-like activity, with dimer **6** being the most active compound, followed by phenol **2** and oxime **7**.

Received 29th November 2024,  
Accepted 16th January 2025

DOI: 10.1039/d4ob01942c

rscl.li/obc

## Introduction

Selenium was discovered in 1817 by the Swedish chemists Berzelius and Gahn, but the organoselenium chemistry only gained momentum after the discovery of selenoxide elimination by Karl B. Sharpless, a syn elimination similar to sulfoxide and nitroxide pyrolysis.<sup>1,2</sup> Although initially considered a toxin for humans, selenium is now recognized as an essential micronutrient due to its incorporation, mostly in the form of selenocysteine, in a number of enzymes that play an important role in the antioxidant defense of cells. The two main groups of selenoenzymes are glutathione peroxidases, which catalyse the decomposition of peroxides by glutathione, and thioredoxin reductases.<sup>3</sup> Selenoproteins are believed to prevent oncogene activation and cancer cell differentiation, and may also interfere with the tumour microenvironment, influencing cancer progression through the activation of inflammatory and immune responses.

The interest in the organoselenium chemistry has significantly increased due to the discovery that these compounds can mimic the effect of glutathione peroxidase (GPx) and reproduce its catalytic activity, thus operating as strong

antioxidants.<sup>4–6</sup> Moreover, a significant number of selenium compounds show antitumor, antimicrobial, and antiviral properties and have been proposed as promising agents for cancer chemoprevention and treatment.<sup>7</sup>

Considerable efforts have been made in the synthesis of selenoderivatives of natural products such as terpenoids, coumarins, steroids or vitamins, since this has been shown to generate enhanced or synergistic pharmacological activities.<sup>8</sup> We have synthesised selenoderivatives of chrysin and tetramethylquercetin with improved antioxidant activity and cytotoxicity, exhibiting a high differential behavior toward malignant and nonmalignant cells.<sup>9</sup> This difference in toxicity led us to further investigate organoselenium compounds derived from other natural compounds. This work reports the formation of selenophene derivatives by the reaction of the naturally occurring terpene (–)-carvone with SeBr<sub>2</sub>. Most syntheses of selenophenes involve the reaction of a selenium electrophile or nucleophile with an acyclic precursor containing a  $\pi$ -system, typically a diene or a diyne, in either one or, most frequently, two steps.<sup>10,11</sup> In the one-pot reaction described here, the  $\pi$ -system reacting with the selenium electrophile comprises an alkene and an enol.

## Results and discussion

### Synthesis of mentoselenophenone 1

The reaction of (–)-carvone with SeBr<sub>2</sub> in CH<sub>2</sub>Cl<sub>2</sub> produced mainly mentoselenophenone **1** as a racemic mixture, together with minor amounts of the fully aromatic phenols **2** and **3** (Scheme 1 and Table 1, entries 1 and 2). The structure of **1** was confirmed by single crystal X-ray diffraction data. The reaction is slow and continues after the total consumption of carvone,

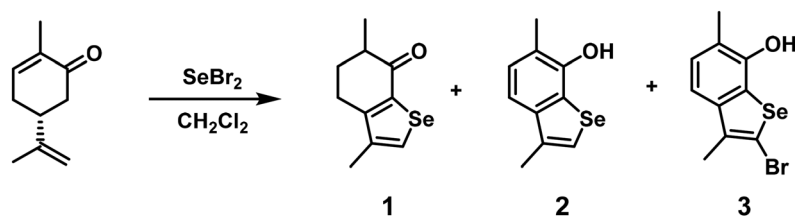
<sup>a</sup>Centro de Química Estrutural, Institute of Molecular Sciences, Departamento de Engenharia Química, Instituto Superior Técnico, Universidade de Lisboa, Av. Rovisco Pais, 1049-001 Lisboa, Portugal. E-mail: jptelo@tecnico.ulisboa.pt

<sup>b</sup>Associação do Instituto Superior Técnico para a Investigação e Desenvolvimento (IST-ID), Avenida António José de Almeida, 12, 1000-043 Lisboa, Portugal

† Electronic supplementary information (ESI) available. CCDC 2394794–2394796. For ESI and crystallographic data in CIF or other electronic format see DOI: <https://doi.org/10.1039/d4ob01942c>

‡ Current address: Escola Superior de Tecnologia do Barreiro, Instituto Politécnico de Setúbal, Rua Américo da Silva Marinho, 2839–001 Barreiro, Portugal.





Scheme 1

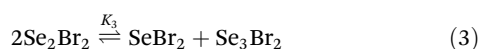
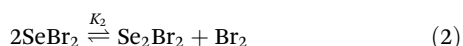
Table 1 Optimization of the reaction of (–)-carvone with Se and Br<sub>2</sub>

Entry	Solvent	Equivalents Se	Equivalents Br <sub>2</sub>	Time (days)	1 <sup>a</sup>	2 <sup>a</sup>	3 <sup>a</sup>
1	CH <sub>2</sub> Cl <sub>2</sub>	1.0	1.0	2	32%	9%	4%
2	CH <sub>2</sub> Cl <sub>2</sub>	1.0	1.0	3	40%	14%	8%
3	CH <sub>2</sub> Cl <sub>2</sub>	2.0	1.0	2	44%	8%	—
4	CH <sub>2</sub> Cl <sub>2</sub>	2.0	1.0	3	<b>49%</b>	9%	1%
5	CH <sub>2</sub> Cl <sub>2</sub>	2.0	1.0	4	43%	12%	4%
6	CH <sub>2</sub> Cl <sub>2</sub>	3.0	1.0	3	23%	10%	—
7	CHCl <sub>3</sub>	2.0	1.0	1	41%	10%	4%
8	CHCl <sub>3</sub>	2.0	1.0	2	<b>50%</b>	10%	4%
9	CHCl <sub>3</sub>	2.0	1.0	3	40%	13%	6%
10	CHCl <sub>3</sub>	2.0	2.0	3	16%	38%	4%
11	C <sub>6</sub> H <sub>6</sub>	2.0	1.0	2	35%	27%	3%
12	C <sub>6</sub> H <sub>6</sub>	2.0	2.0	3	—	<b>56%</b>	5%

<sup>a</sup> Yields reflect the amount of isolated product, but the yields of 2 and 3 were computed from the isolated mass of the phenol mixture and the ratio of 2/3 determined by <sup>1</sup>H NMR analysis.

as shown by the constant release of gaseous HBr. By stopping the reaction after a few hours, an inseparable complex mixture is obtained. Carvone isomerizes into carvacrol in the presence of strong acids like HBr,<sup>12</sup> and since two equivalents of HBr are produced in the reaction, the absence of carvacrol among the products suggests that the slow step is not the initial reaction of carvone with SeBr<sub>2</sub>.

By adding equimolar amounts of molecular bromine and elemental selenium, the dark red-brown color of selenium dibromide appears immediately (eqn (1)). However, it has been shown both spectrophotometrically and by <sup>77</sup>Se NMR that, in solution, selenium dibromide disproportionates into Se<sub>2</sub>Br<sub>2</sub> and bromine (eqn (2)), with  $K_2 = 0.0252$  in CCl<sub>4</sub> and  $K_2 = 0.14$  in acetonitrile.<sup>13,14</sup> The latter value might explain why the reaction does not proceed in acetonitrile and other polar solvents. Se<sub>2</sub>Br<sub>2</sub> is also involved in further disproportionation equilibria, as shown in eqn (3) ( $K_3 = 2.2 \times 10^{-4}$  in CH<sub>2</sub>Cl<sub>2</sub>).



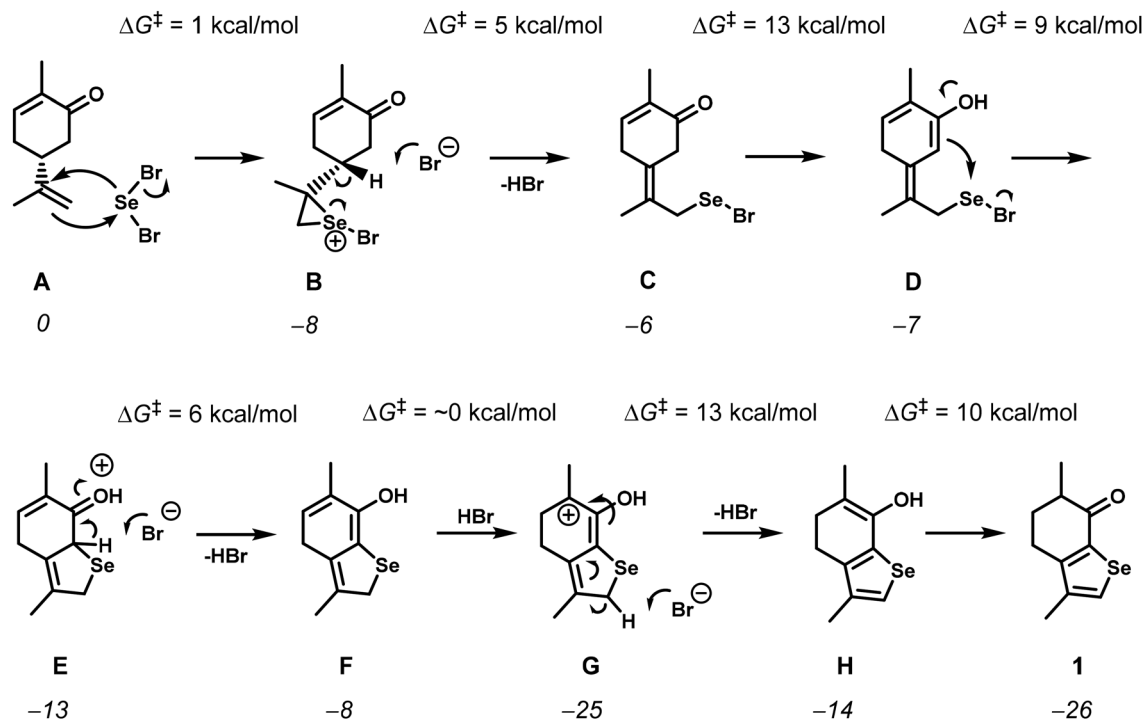
This shows that free bromine is always present in the reaction mixture, which accounts for the presence of 2 and 3. Phenol 2 is produced by the  $\alpha$ -bromination of ketone 1, followed by HBr elimination (see below). Aromatic bromination

of 2 in the activated selenophene ring produces 3. Consistently, using two equivalents of selenium improves the yield of 1 (entries 3–5) by reducing the concentration of free Br<sub>2</sub> (eqn (1)), but above this ratio, the yield decreases (entry 6). In this case, the main species in solution should be Se<sub>2</sub>Br<sub>2</sub>, but the reactive (electrophilic) selenium compound is probably still SeBr<sub>2</sub>. The reaction is somewhat faster in chloroform, with similar yields (entries 7–9). It is also faster in benzene (entry 11), but with a lower yield of 1 and a higher yield of phenol 2.

The reaction of (–)-carvone with SeBr<sub>2</sub> occurs through the addition of the exocyclic double bond and the ketone enol to the selenium electrophile, but the unusual migration of the endocyclic double bond to the selenophene moiety made us study the mechanism by DFT calculations<sup>15</sup> (see the ESI† for computational details). A simplified version of the mechanism is presented in Scheme 2, while the complete free energy profile can be found in the ESI (Fig. S1–S4†).

The reaction starts with the addition of selenium dibromide to the isopropenyl group double bond, forming the usual seleniranion **B**,<sup>16</sup> with a negligible barrier of only 1 kcal mol<sup>–1</sup>. The alternative would be the addition to the enol double bond, but this would have a barrier of 14 kcal mol<sup>–1</sup>, primarily due to the costly energy conversion from the keto to the enol form of carvone (Fig. S5†). In fact, the enol intermediate (**I** in Fig. S5†) is 13 kcal mol<sup>–1</sup> less stable than the corresponding keto form, present in **A**. The seleniranion ion **B** eliminates HBr to yield the exocyclic double bond in **C**, in a simple process with a barrier of 5 kcal mol<sup>–1</sup>. The next two





**Scheme 2** Simplified mechanism for the formation of **1** calculated using DFT. Free energy values of the intermediates (italics) and barriers ( $\Delta G^\ddagger$ ) are given in kcal mol<sup>-1</sup>.

steps are the enolization of the ketone and the attack of the enol on the selenium atom to yield the cyclic selenide **F**. The enolization of **C** has a barrier of 13 kcal mol<sup>-1</sup> and yields intermediate **D**, followed by the attack of the C=C double bond of the enol to the Se atom and the consequent formation of the 5-member ring in intermediate **E**, which is subsequently deprotonated to give **F**. The formation of the Se-C bond is the rate determining step of the mechanism. The overall barrier of the reaction is 18 kcal mol<sup>-1</sup>, measured from **C**, the protonated ketone with the exocyclic double bond (Fig. S1†), to the transition state for the formation of the Se-C bond, **D**<sup>‡</sup> (Fig. S2†). The migration of the C5-C6 double bond to the selenophene ring is achieved by protonation of the enol **F** at C5, followed by deprotonation at the C-atom adjacent to Se in the cycle, resulting in the enol intermediate **H**. The series of steps, from **E** to **H**, present low free energy barriers, with the highest one (13 kcal mol<sup>-1</sup>) corresponding to C-H deprotonation, from **G** to **H**. The reaction is completed through tautomerization from the enol in intermediate **H** to the keto form in the final product, **1**. This is, again, an easy step with a barrier of 10 kcal mol<sup>-1</sup>. Importantly, all proton transfer steps, namely the enolization processes, are facilitated by the high concentration of HBr released in the previous steps. The overall reaction from **A** to **1** is highly exergonic with  $\Delta G_R = -26$  kcal mol<sup>-1</sup>.

### Synthesis of mentoselenophenone derivatives

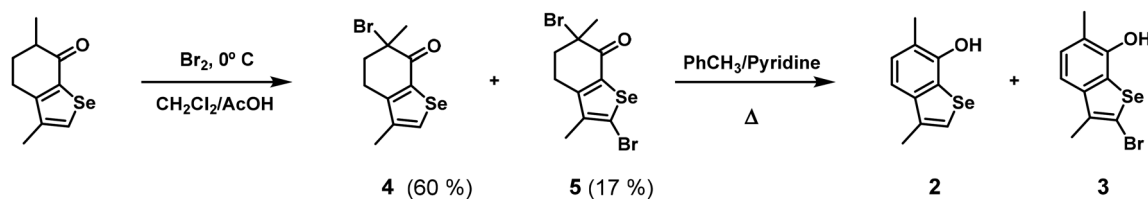
As stated before, the presence of free bromine in the reaction mixture produces phenol **2** by  $\alpha$ -bromination of ketone **1** and elimination of HBr (Scheme 1). Further aromatic bromination

of **2** on the activated selenophene ring yields phenol **3**. With two equivalents of bromine, the yield of the two aromatic phenols increases, as expected (Table 1, entries 10 and 12). This allows the isolation of phenol **2** as the main product in benzene (entry 12).

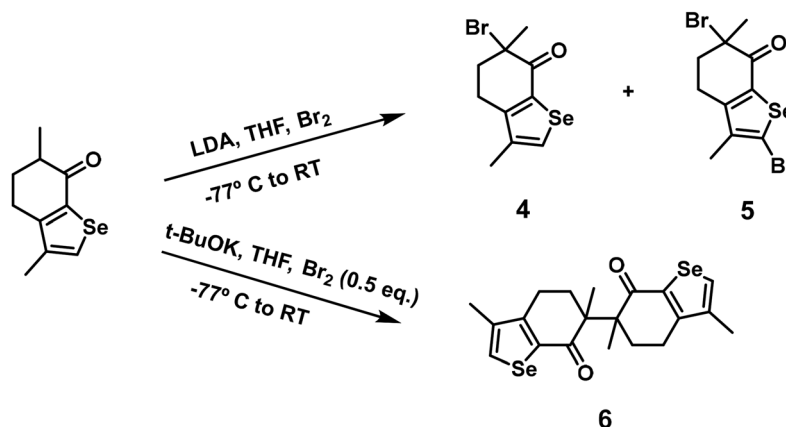
Improved yields of **2** and **3** were obtained upon preparation of their  $\alpha$ -bromo ketone precursors by acid-catalysed bromination of mentoselenophenone **1** at 0 °C (Scheme 3). Both products **4** and **5** are stable enough for characterization, including crystal structure determination from single crystal X-ray diffraction data, in the case of **4**. Nevertheless, some decomposition was noticed for long storage times, even under cold conditions and a nitrogen atmosphere, as both compounds develop a darker yellow hue. Refluxing the product mixture in toluene/pyridine yields **2** and **3** quantitatively.

The same mixture of **4** and **5** was also obtained in similar yields by bromination of **1** under base catalysis with LDA in THF, but when the same reaction was carried out with potassium *t*-butoxide, the products contained a significant portion of dimer **6** (Scheme 4). Dimer **6** could be isolated in 78% yield by using one-half equivalents of Br<sub>2</sub>. X-ray crystallography shows **6** to be a racemic mixture. There is no evidence for the formation of the *meso* stereoisomer. The potassium enolate of **1** probably reacts with the tertiary  $\alpha$ -bromo ketone, which might be one of the few examples of an S<sub>N</sub>2-type reaction on a tertiary carbon atom.<sup>17-19</sup> Having the structure of the dimer, the reaction path for an S<sub>N</sub>2-type reaction was studied by DFT calculations (Fig. S6 in the ESI†). Surprisingly, the transition state was found to be only 5.6 kcal mol<sup>-1</sup> above the energy of the





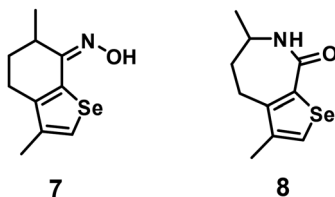
Scheme 3



Scheme 4

separated reactants, an activation barrier that is compatible with the reaction conditions. However, a radical  $S_{\text{NR}}1$ -type mechanism cannot be excluded, and further studies would be needed to unequivocally determine the mechanism of this reaction.

To maximize the number of available selenium derivatives with potential biological effects, the oxime derivative of **1** was prepared in 76% yield. Following treatment of oxime **7** with thionyl chloride, its Beckmann rearrangement product lactam **8** was obtained in 60% yield. The structure of the lactam shows that the oxime has a *Z* configuration, since the group migrating to the nitrogen atom in the Beckmann rearrangement is the one anti-periplanar to the hydroxyl group.



### Crystal structures

Single crystal X-ray diffraction analysis confirmed the structure of compounds **1**, **4** and **6** without ambiguity (Fig. 1). Relevant details of the X-ray data analysis are displayed in Table S1.†

Bond lengths and angles are comparable in the three molecules and are within the expected range, as judged from extensive analysis of the values included in the CSD.<sup>20</sup> In compound **1**, the selenophene ring can be considered planar, according to the very small values of deviation from the plane of all the five atoms. In compounds **4**, these values are slightly larger, but the root-mean-square deviation is still small enough for the ring to be considered quasi-planar. In **6**, one of the rings has a slightly higher deviation from planarity, but it is still very close to planar (see Fig. 1 and Table S2†). Furthermore, in compound **6**, the angle between two Se ring planes is 70.76 (6)°.

The bond lengths of all bonds forming the five-membered rings in the three compounds are in good agreement with the planar geometry of these rings. The values of Se(1)–C(2) and Se(1)–C(7a) in the three compounds are similar to the mean value reported in the literature for Se–C<sub>sp<sup>2</sup></sub> bonds (1.893 Å). The C–C bonds show values typical of conjugated bonds connecting C<sub>sp<sup>2</sup></sub> atoms (see Table S3†).<sup>21</sup>

The three compounds crystallize in centrosymmetric space groups ( $P2_1/n$  for **1** and **4** and  $P\bar{1}$  for **6**), which means they have inversion symmetry. This symmetry precludes the crystallization of a single enantiomer, as chiral molecules do not have an inversion centre. Therefore, these compounds are racemic mixtures, with equal amounts of left- and right-handed enantiomers coexisting in the crystal lattice. These molecules pack in such a way that each enantiomer is paired with its mirror



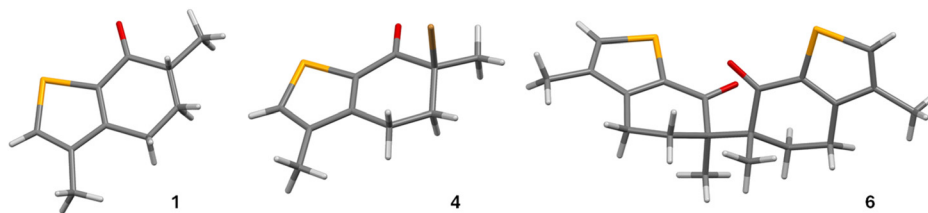


Fig. 1 Diagrams of the molecular structures of compounds **1**, **4** and **6** (atom colour code: Se, yellow; Br, brown; O, red; C, grey; H, light grey).

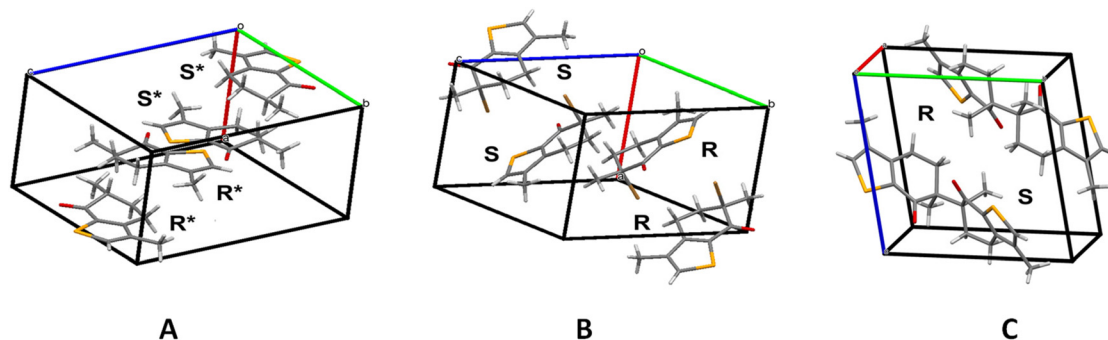


Fig. 2 Unit cell of compounds **1** (A), **4** (B) and **6** (C) depicting the presence of both left- and right-handed enantiomers (axis: red – a; green – b; blue – c).

image, effectively cancelling out chirality at the macroscopic level.

Compounds **1** and **4** crystallize in the  $P2_1/n$  space group, indicating that the molecules are organized with a glide plane and a two-fold screw axis along with an inversion centre. The molecules are arranged such that each chiral molecule has a corresponding molecule of the opposite chirality, leading to a centrosymmetric arrangement in the unit cell, in which each enantiomer occupies specific sites related by symmetry operations (Fig. 2). In **6**, which crystallizes in the  $P\bar{1}$  space group, molecules are organized in pairs of opposite enantiomers related by the inversion centre within the crystal, which also leads to a centrosymmetric arrangement (Fig. 2).

### GPx-like activity

Selenocompounds can act as antioxidants by reacting with peroxides and be regenerated by glutathione, thus mimicking the catalytic activity of the selenoenzyme GPx. The GPx-like activity of selenocompounds **1–3** and **6** was assessed using the method of Iwaoka *et al.*,<sup>22</sup> where dithiothreitol (DTT<sup>red</sup>) is used as a reducing cofactor instead of glutathione. The rate of the reaction was monitored by measuring the increase of the disulfide form (DTT<sup>ox</sup>) using <sup>1</sup>H NMR spectroscopy in CD<sub>3</sub>OD. Compounds **4** and **5** are too labile in solution and were not considered in this study. The results are shown in Fig. 3.

To compare the catalytic activity of the different compounds, we calculated the time necessary to oxidize 50% of DTT<sup>red</sup>,  $t_{1/2}$ . Both phenol **2** ( $t_{1/2}$  = 42 min) and oxime **7** ( $t_{1/2}$  = 52 min) exhibit higher catalytic activity than mentoselenophenone **1** ( $t_{1/2}$  = 71 min). The presence of extra OH redox units in

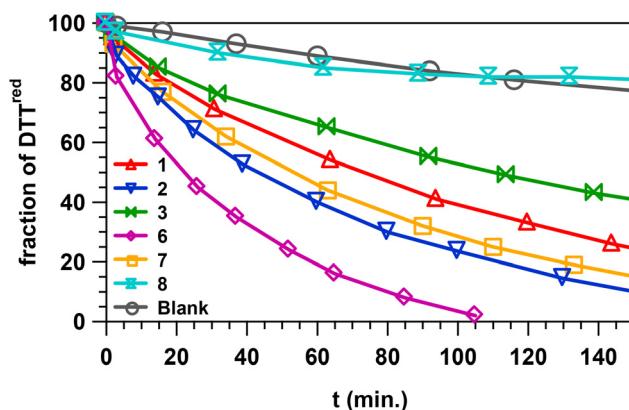


Fig. 3 Percentage of DTT<sup>red</sup> as a function of time in the oxidation of DTT<sup>red</sup> (0.1 M) with H<sub>2</sub>O<sub>2</sub> (0.1 M) in the absence (blank) or in the presence of several selenophene catalysts (0.01 M).

both **2** and **7** probably facilitates the catalytic cycle of the selenium atom. In the case of **7**, the H atom of the oxime OH group is directly accessible by the selenium atom due to spatial proximity. Phenol **3** has a lower activity ( $t_{1/2}$  = 110 min) due to the electron withdrawing effect of the bromo atom, making the oxidation of the molecule more difficult. The most active selenocompound is dimer **6**, with  $t_{1/2}$  = 20 min. The presence of two Se atoms and, possibly, the interaction between the two selenophenone moieties, where the two carbonyls are closely positioned in the crystal structure, might explain this result. Surprisingly, lactam **8**, although structurally similar to the other selenocompounds, had no catalytic effect





on the oxidation of DTT<sup>red</sup>. Although the experiments have been repeated twice, we think that the fluctuation of the curve for **8** compared to the blank results from experimental error.

## Conclusions

Mentoselenophenone **1** is the main product of the one-pot reaction of (–)-carvone with SeBr<sub>2</sub>, yielding phenols **2** and **3** as minor products. The synthesis of **1** proceeds through the reaction of the exocyclic carbon–carbon double bond and the endocyclic enol of (–)-carvone with selenium bromide. Although in selenoxide elimination, the β-ketoselenide precursor is usually prepared by the reaction of an enol or enolate with selenium bromide, the reactivity of enols towards selenium electrophiles has not been much used in the synthesis of selenophenes or other selenium compounds, and we think this might be an area worth exploring.

Several derivatives of compound **1** have also been prepared, and their GPx-like catalytic activity is measured. All but lactam **8** have GPx-like activity, with dimer **6** being the most active.

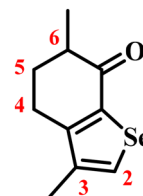
## Experimental

### Starting materials

(–)-Carvone was prepared from (+)-limonene according to known procedures.<sup>23</sup> Commercial molecular sieves were dried at 200 °C under vacuum before use and kept under nitrogen. Dichloromethane was dried over molecular sieves. Chloroform was freed from ethanol by shaking with concentrated sulphuric acid, washed with water, dried with anhydrous magnesium sulphate, distilled, and kept for short periods over molecular sieves. Benzene was dried by refluxing with sodium wire using the blue benzophenone radical anion as an indicator, distilled, and kept under nitrogen. All other reactants were commercially available and used without purification.

**Mentoselenophenone 1 (3,6-dimethyl-5,6-dihydrobenzo[*b*]selenophen-7(4*H*)-one).** A solution of bromine (0.23 mL, 4.47 mmol) in 10 mL of dry CH<sub>2</sub>Cl<sub>2</sub> was added dropwise to a suspension of black selenium powder (706 mg, 8.95 mmol) in dry CH<sub>2</sub>Cl<sub>2</sub> (10 mL) under a nitrogen atmosphere. The resulting mixture was stirred for 1 h at room temperature. After this, 0.7 mL of (–)-carvone (672 mg, 4.47 mmol) was added and the mixture was stirred for 3 days. The system was purged with nitrogen a few times to exhaust the excess of gaseous HBr. The liquid was then decanted and the precipitated selenium was washed twice with 10 mL of CH<sub>2</sub>Cl<sub>2</sub>. A solution of 1.1 g of KOH in 5 mL of water was added to the combined CH<sub>2</sub>Cl<sub>2</sub> extracts and the mixture was heated under reflux in a water bath with strong stirring for 15 minutes. This converts the small amounts of α-bromo ketones still present into phenols **2** and **3**. After cooling, the mixture was transferred to a separatory funnel and extracted first with 20 mL of water, twice with 25 mL of 1 M KOH and finally with water. The aqueous extracts were washed with 10 mL of CH<sub>2</sub>Cl<sub>2</sub> and set aside for further iso-

lation of **2** and **3**. The combined extracts of CH<sub>2</sub>Cl<sub>2</sub> were dried and evaporated under vacuum to yield an oil that crystallises on cooling. This was dissolved in a minimum amount of cyclohexane, filtered through a short column of silica gel (8 cm height, 1.3 cm in diameter) and the column was washed with 300 mL of cyclohexane (*n*-hexane or light petroleum can also be used, although the amount of solvent might have to be adjusted). If more solvent is to be used, purity should be checked by TLC. Evaporation of the solvent yields 500 mg (49% yield) of mentoselenophenone **1**. Recrystallization from a minimum amount of *n*-hexane affords white crystals of analytical purity with a sweet musky odour. Slow evaporation from *n*-octane yielded crystals suitable for X-ray diffraction.



Mp: 90–91 °C (from *n*-hexane); TLC: *R*<sub>f</sub> = 0.22 (toluene); <sup>1</sup>H NMR (400 MHz, CDCl<sub>3</sub>): δ = 7.88 (s, H; 2-CH), 2.78–2.71 (dt, H, *J* = 17.2 Hz, *J* = 4.7 Hz; 4-CH<sub>2</sub>), 2.65–2.58 (m, 2H; 4-CH<sub>2</sub>, 6-CH), 2.28–2.23 (m, H; 5-CH<sub>2</sub>), 2.14 (s, 3H; 3-CCH<sub>3</sub>), 1.99–1.89 (m, H; 5-CH<sub>2</sub>), 1.26 ppm (d, 3H; *J* = 6.9 Hz; 6-CCH<sub>3</sub>); <sup>13</sup>C NMR (400 MHz, CDCl<sub>3</sub>): δ = 195.9, 154.2, 141.5, 139.9, 134.0, 41.6, 32.2, 25.9, 16.3, 15.4 ppm; HR-EI/MS: *m/z* (int.) calcd for C<sub>10</sub>H<sub>12</sub>OSe [M + H]<sup>+</sup> 229.0126 (100); found 229.0133 (100).

**3,6-Dimethylbenzo[*b*]selenophen-7-ol (2) and 2-bromo-3,6-dimethylbenzo[*b*]selenophen-7-ol (3).** A solution of bromine (0.23 mL, 4.47 mmol) in 10 mL of benzene was added dropwise to a suspension of selenium powder (706 mg, 8.95 mmol) in benzene (10 mL) under nitrogen. The resulting mixture was stirred for 1 h at room temperature. After this, 0.7 mL of (–)-carvone (672 mg, 4.47 mmol) was added and the mixture was stirred under nitrogen. After 48 h, an additional amount of bromine (0.23 mL, 4.47 mmol) was directly added to the solution. The system was purged with nitrogen a few times during the reaction. After another 48 h, the mixture was refluxed for 15 minutes to exhaust the excess of HBr. After cooling, the selenium powder was decanted, 1.5 mL of dry pyridine was added to the benzene solution and the mixture was refluxed for 24 h. The cold solution was washed twice with 1 M H<sub>2</sub>SO<sub>4</sub>, followed by water, and dried over anhydrous MgSO<sub>4</sub>. After evaporation of the solvent, the crude oil was purified by flash column chromatography with dry silica gel (*n*-hexane). Phenol **3** was eluted first (80 mg, 6%), followed by phenol **2** (560 mg, 56%).

Alternatively, both products can be obtained in low yield from the aqueous extracts obtained in the synthesis of **1**. These were made acidic with concentrated HCl and extracted three times with 25 mL of CH<sub>2</sub>Cl<sub>2</sub>. The combined organic fraction was dried and evaporated, and the mixture was separated as described above.



2: mp = 98–99 °C (needles from *n*-hexane); TLC:  $R_f$  = 0.34 (toluene);  $^1\text{H}$  NMR (400 MHz,  $\text{CDCl}_3$ ):  $\delta$  = 7.46 (s, H; 2-CH), 7.24 (d, H,  $J$  = 7.9 Hz; 4-CH), 7.18 (d, H,  $J$  = 8.0 Hz; 5-CH), 4.93 (s, H; OH), 2.37 (s, 3H; 6- $\text{CCH}_3$ ), 2.36 ppm (s, 3H; 3- $\text{CCH}_3$ );  $^{13}\text{C}$  NMR (400 MHz,  $\text{CDCl}_3$ ):  $\delta$  = 150.4, 142.8, 135.9, 128.7, 128.3, 122.4, 117.4, 116.4, 16.2, 15.5 ppm; HR-EI/MS:  $m/z$  (int.) calcd for  $\text{C}_{10}\text{H}_{10}\text{OSe}$   $[\text{M} + \text{H}]^+$  226.9970 (100); found 226.9965 (100).

3: mp = 105–106 °C; TLC:  $R_f$  = 0.45 (toluene);  $^1\text{H}$  NMR (400 MHz,  $\text{CDCl}_3$ ):  $\delta$  = 7.16 (AB q, 2H; 4-CH, 5-CH), 4.94 (s, H; OH), 2.33 (s, 3H; 6- $\text{CCH}_3$ ), 2.29 ppm (s, 3H; 3- $\text{CCH}_3$ );  $^{13}\text{C}$  NMR (400 MHz,  $\text{CDCl}_3$ ):  $\delta$  = 149.5, 141.6, 135.6, 128.5, 128.3, 117.9, 116.5, 111.2, 15.4, 15.0 ppm; HR-EI/MS:  $m/z$  (int.) calcd for  $\text{C}_{10}\text{H}_9\text{BrOSe}$   $[\text{M} + \text{H}]^+$  304.9072 (100); found 304.9069 (100).

**6-Bromo-3,6-dimethyl-5,6-dihydrobenzo[*b*]selenophen-7(4*H*)-one (4) and 2,6-dibromo-3,6-dimethyl-5,6-dihydrobenzo[*b*]selenophen-7(4*H*)-one (5).** A solution of 450 mg of **1** (1.98 mmol) in 5 ml of  $\text{CH}_2\text{Cl}_2$  and 5 ml of acetic acid was cooled in an ice bath. To this cold solution, 0.11 ml of  $\text{Br}_2$  (2.1 mmol) in 5 ml of  $\text{CH}_2\text{Cl}_2$  was added dropwise with stirring, and the mixture was stirred at room temperature for 12 h. After this time, the strong brown colour faded to light orange, and the release of HBr mostly ceased. The solution was then diluted with an additional 10 ml of dichloromethane and washed with ice-cold water, twice with a cold solution of sodium bicarbonate (2 × 30 ml) and again with cold water. After being dried over anhydrous magnesium sulphate, the solution was evaporated under vacuum at 30 °C. The residue was purified by flash chromatography with dry silica gel (*n*-hexane) to yield 130 mg of **5** (17%), followed by 365 mg of **4** (60%). Alternatively, the residue can be refluxed in toluene/pyridine as described above to give phenols **2** and **3** quantitatively.

**4:** mp = 86–87 °C (from *n*-hexane);  $R_f$  = 0.53 (toluene);  $^1\text{H}$  NMR (400 MHz,  $\text{CDCl}_3$ ):  $\delta$  = 7.99 (s, H; 2-CH), 2.88–2.67 (m, 2H; 4- $\text{CH}_2$ ), 2.62–2.55 (m, H; 5- $\text{CH}_2$ ), 2.29–2.19 (m, H; 5- $\text{CH}_2$ ), 2.17 (s, 3H; 6- $\text{CCH}_3$ ), 2.01 ppm (s, 3H; 3- $\text{CCH}_3$ );  $^{13}\text{C}$  NMR (400 MHz,  $\text{CDCl}_3$ ):  $\delta$  = 186.8, 153.5, 139.9, 138.4, 136.2, 62.6, 41.0, 27.9, 25.7, 16.6 ppm; HR-EI/MS:  $m/z$  (int.) calcd for  $\text{C}_{10}\text{H}_{11}\text{BrOSe}$   $[\text{M} + \text{H}]^+$  306.9228 (100); found 306.9225 (100).

**5:** mp = 90–91 °C (from *n*-hexane);  $R_f$  = 0.66 (toluene);  $^1\text{H}$  NMR (400 MHz,  $\text{CDCl}_3$ ): 2.88–2.67 (m, 2H; 4- $\text{CH}_2$ ), 2.62–2.55 (m, H; 5- $\text{CH}_2$ ), 2.29–2.19 (m, H; 5- $\text{CH}_2$ ), 2.17 (s, 3H; 6- $\text{CCH}_3$ ), 2.01 ppm (s, 3H; 3- $\text{CCH}_3$ );  $^{13}\text{C}$  NMR (400 MHz,  $\text{CDCl}_3$ ):  $\delta$  = 186.8, 153.5, 139.9, 138.4, 136.2, 62.6, 41.0, 27.9, 25.7, 16.6 ppm; HR-EI/MS:  $m/z$  (int.) calcd for  $\text{C}_{10}\text{H}_{10}\text{Br}_2\text{OSe}$   $[\text{M} + \text{H}]^+$  386.8316 (100); found 386.8307 (100).

**3,3',6,6'-Tetramethyl-5,5',6,6'-tetrahydro[6,6'-bibenzo[*b*]selenophene]-7,7'(4*H*,4'*H*)-dione (6).** To a solution of 200 mg of **1** (0.88 mmol) in 10 ml of dry THF cooled to –77 °C was added 0.2 g of potassium *tert*-butoxide (1.76 mmol) and the solution was stirred at this temperature for 30 min. After this, 22.7  $\mu\text{L}$  of  $\text{Br}_2$  was added directly to the solution and the reaction mixture was allowed to reach room temperature (4 hours). The mixture was dissolved in 40 ml of ethyl acetate and 40 ml of water and agitated in a separatory funnel. The organic phase was dried over anhydrous magnesium sulphate and evaporated under vacuum. The solid was washed with 5 ml of cold hexane

to yield 155 mg of dimer **6** (78%). An analytical sample could be obtained by filtration through a short column of silica gel (hexane/toluene 1 : 10).

mp = 207–209 °C;  $R_f$  = 0.11 (toluene);  $^1\text{H}$  NMR (400 MHz,  $\text{CDCl}_3$ ):  $\delta$  = 7.59 (s, H; 2-CH), 2.99–3.06 (m, H; 5- $\text{CH}_2$ ), 2.61–2.77 (m, 2H; 4- $\text{CH}_2$ ), 2.13 (s, 3H; 3- $\text{CCH}_3$ ), ~2.12 (m, H; 5- $\text{CH}_2$ ), 1.35 ppm (s, 3H; 6- $\text{CCH}_3$ );  $^{13}\text{C}$  NMR (400 MHz,  $\text{CDCl}_3$ ):  $\delta$  = 198.4, 151.9, 142.3, 139.5, 134.3, 50.2, 32.9, 23.9, 17.7, 16.3 ppm; HR-EI/MS:  $m/z$  (int.) calcd for  $\text{C}_{10}\text{H}_{12}\text{OSe}$   $[\text{M} + \text{H}]^+$  455.00286 (100); found 455.0013 (100).

**(Z)-3,6-Dimethyl-5,6-dihydrobenzo[*b*]selenophen-7(4*H*)-one oxime (7).** A solution of 230 mg of **1** (1 mmol), 120 mg of  $\text{NH}_2\text{OH}\cdot\text{HCl}$  (1.7 mmol), and 0.2 ml of dry pyridine in 10 ml of absolute ethanol was refluxed for 24 h. The mixture was then evaporated under vacuum, and 25 ml of ethyl acetate was added. This solution was washed twice with ice-cold 25 ml of 0.5 M  $\text{H}_2\text{SO}_4$ , followed by water, and dried over anhydrous  $\text{MgSO}_4$ . The solvent was evaporated under vacuum, and the resulting solid was washed twice with 5 ml of warm hexane to yield 184 mg of oxime **7** (76%). Recrystallization from toluene/hexane afforded an analytical sample.

mp = 160–162 °C;  $^1\text{H}$  NMR (400 MHz,  $\text{CDCl}_3$ ):  $\delta$  = 7.85 (s, H; 2-CH), 2.86–2.90 (m, H; 6-CH), 2.62–2.70 (m, 2H; 4- $\text{CH}_2$ ), 2.15 (s, 3H; 3- $\text{CCH}_3$ ), 2.07–2.10 (m, H; 5- $\text{CH}_2$ ), 1.84–1.89 (m, H; 5- $\text{CH}_2$ ), 1.30 ppm (d, 3H;  $J$  = 6.8 Hz; 6- $\text{CCH}_3$ );  $^{13}\text{C}$  NMR (400 MHz,  $\text{CDCl}_3$ ):  $\delta$  = 154.3, 145.4, 137.7, 132.0, 126.0, 34.4, 30.1, 25.0, 18.0, 16.3 ppm; HR-EI/MS:  $m/z$  (int.) calcd for  $\text{C}_{10}\text{H}_{13}\text{NOSe}$   $[\text{M} + \text{H}]^+$  244.0235 (100); found 244.0190 (100).

**3,6-Dimethyl-4,5,6,7-tetrahydro-8*H*-selenopheno[2,3-*c*]azepin-8-one (8).** A solution of 0.12 ml (0.20 g, 1.65 mmol) of freshly distilled thionyl chloride in 5 ml of anhydrous THF was added dropwise with agitation to a solution of 100 mg (0.41 mmol) of oxime **7** in 5 ml of anhydrous THF cooled in an ice bath. The mixture was stirred for 30 min at 0 °C. After this, the ice bath was removed, and the mixture was stirred for an additional 30 min at room temperature. The solvent was then removed by evaporation under vacuum. The solid was briefly stirred with

Table 2 Crystallographic details for compounds **1**, **4** and **6**

	<b>1</b>	<b>4</b>	<b>6</b>
Crystal system	Monoclinic	Monoclinic	Triclinic
Space group	$P2_1/n$	$P2_1/n$	$P\bar{1}$
<i>a</i> (Å)	7.300(7)	7.767(3)	10.0831(14)
<i>b</i> (Å)	10.3528(9)	10.906(4)	10.4303(15)
<i>c</i> (Å)	12.964(12)	12.122(4)	10.7237(16)
$\alpha$ (°)	90	90	71.641(6)
$\beta$ (°)	91.02	90.88(2)	70.303(6)
$\gamma$ (°)	90	90	63.501(6)
<i>V</i> (Å <sup>3</sup> )	980.1(15)	1026.7(6)	932.0(2)
<i>Z</i>	4	4	2
GoF	1.019	1.022	1.012
Final <i>R</i> indices <sup>a,b</sup> [ $I > 2\sigma(I)$ ]	$R_1 = 0.0650$		
$wR_2 = 0.1539$	$R_1 = 0.0376$		
$wR_2 = 0.0827$	$R_1 = 0.0561$		
$wR_2 = 0.0915$			

$$^a R_1 = \sum ||F_o| - |F_c|| / \sum |F_o|. \quad ^b wR_2 = [\sum [w(F_o^2 - F_c^2)^2] / \sum [w(F_o^2)^2]]^{1/2}.$$



ice water, filtered, dried, and washed twice with 10 ml portions of hexane to yield 60 mg (60%) of lactam **8**.

Mp = 144–145 °C;  $^1\text{H}$  NMR (400 MHz,  $\text{CDCl}_3$ ):  $\delta$  = 7.73 (s, H; 2-CH), 5.89 (s, H; NH), 3.59–3.60 (m, H; 6-CH), 2.70–2.77 (m, 2H; 4-CH<sub>2</sub>), 2.08–2.13 (m, H; 5-CH<sub>2</sub>), 2.11 (s, 3H; 3-CCH<sub>3</sub>), 1.98–2.02 (m, H; 5-CH<sub>2</sub>), 1.31 ppm (d, 3H;  $J$  = 6.7 Hz; 6-CCH<sub>3</sub>);  $^{13}\text{C}$  NMR (400 MHz,  $\text{CDCl}_3$ ):  $\delta$  = 166.0, 144.4, 141.4, 140.5, 131.0, 48.6, 34.5, 30.4, 22.2, 18.0 ppm; HR-EI/MS:  $m/z$  (int.) calcd for  $\text{C}_{10}\text{H}_{13}\text{NOSe}$   $[\text{M} + \text{H}]^+$  244.0235 (100); found 244.0190 (100).

### Single crystal X-ray diffraction

X-ray crystallographic data for compounds **1**, **4** and **6** (CCDC 2394794–2394796†) were collected from single crystals using an area detector diffractometer (Bruker AXS-KAPPA APEX II) at room temperature with graphite-monochromated Mo K $\alpha$  ( $\lambda$  = 0.71073 Å) radiation. Further details on data collection and structure determination and refinement are available in the ESI† Table 2 lists the main crystallographic details, and complete crystallographic details are provided in Table S1 (see the ESI†).

### Data availability

Crystallographic data for compounds **1**, **4** and **6** have been deposited with the Cambridge Crystallographic Data Centre (CCDC 2394794–2394796†).

### Conflicts of interest

There are no conflicts to declare.

### Acknowledgements

We thank the Fundação para a Ciência e a Tecnologia (FCT), I/P/MCTES, through national funds PIDDAC – CQE UIDB/00100/2020 (<https://doi.org/10.5449/UIDP/00100/2020>) and UIDP/00100/2020 (<https://doi.org/10.54499/UIDB/00100/2020>), and IMS, the Associated Laboratory, funded by Project LA/P/0056/2020 (<https://doi.org/10.54499/LA/P/0056/2020>). VA acknowledges FCT for contract CEECIND/00283/2018/CP1572/CT0004 (<https://doi.org/10.54499/CEECIND/00283/2018/CP1572/CT0004>).

### References

- 1 D. N. Jones, D. Mundy and R. D. Whitehouse, Steroidal selenoxides diastereoisomeric at selenium; syn-elimination, absolute configuration, and optical rotatory dispersion characteristics, *J. Chem. Soc., Chem. Commun.*, 1970, 86–87, DOI: [10.1039/C29700000086](https://doi.org/10.1039/C29700000086).
- 2 K. B. Sharpless, M. W. Young and R. F. Lauer, Reactions of Selenoxides – Thermal syn-elimination and  $\text{H}_2\text{O}$ -18 Exchange, *Tetrahedron Lett.*, 1973, 1979–1982, DOI: [10.1016/S0040-4039\(01\)96098-8](https://doi.org/10.1016/S0040-4039(01)96098-8).
- 3 L. B. Maia, B. K. Maiti, I. Moura and J. J. G. Moura, Selenium-More than Just a Fortuitous Sulfur Substitute in Redox Biology, *Molecules*, 2024, **29**, 120, DOI: [10.3390/molecules29010120](https://doi.org/10.3390/molecules29010120).
- 4 V. Nascimento, E. E. Alberto, D. W. Tondo, D. Dambrowski, M. R. Detty, F. Nome and A. L. Braga, GPx-Like Activity of Selenides and Selenoxides: Experimental Evidence for the Involvement of Hydroxy Perhydroxy Selenane as the Active Species, *J. Am. Chem. Soc.*, 2012, **134**, 138–141, DOI: [10.1021/ja209570y](https://doi.org/10.1021/ja209570y).
- 5 N. V. Barbosa, C. W. Nogueira, P. A. Nogara, A. F. de Bem, M. Aschner and J. B. T. Rocha, Organoselenium compounds as mimics of selenoproteins and thiol modifier agents, *Metallomics*, 2017, **9**, 1703, DOI: [10.1039/c7mt00083a](https://doi.org/10.1039/c7mt00083a).
- 6 J. M. Anghinoni, P. T. Birmann, M. J. da Rocha, C. S. Gomes, M. J. Davies, C. A. Brüning, L. Savegnago and E. J. Lenardão, Recent Advances in the Synthesis and Antioxidant Activity of Low Molecular Mass Organoselenium Molecules, *Molecules*, 2023, **28**, 7349, DOI: [10.3390/molecules28217349](https://doi.org/10.3390/molecules28217349).
- 7 D. Bartolini, L. Sancineto, A. Fabro de Bem, K. D. Tew, C. Santi, R. Radi, P. Toquato and F. Galli, Selenocompounds in Cancer Therapy: An Overview, *Adv. Cancer Res.*, 2017, **136**, 259–302, DOI: [10.1016/bs.acr.2017.07.007](https://doi.org/10.1016/bs.acr.2017.07.007).
- 8 W. Hou and H. Xu, Incorporating Selenium into Heterocycles and Natural Products—From Chemical Properties to Pharmacological Activities, *J. Med. Chem.*, 2022, **65**, 4436–4456, DOI: [10.1021/acs.jmedchem.1c01859](https://doi.org/10.1021/acs.jmedchem.1c01859).
- 9 I. L. Martins, C. Charneira, V. Gandin, J. L. Ferreira da Silva, G. C. Justino, J. P. Telo, A. J. S. C. Vieira, C. Marzano and A. M. M. Antunes, Selenium-Containing Chrysin and Quercetin Derivatives: Attractive Scaffolds for Cancer Therapy, *J. Med. Chem.*, 2015, **58**, 4250–4265, DOI: [10.1021/acs.jmedchem.5b00230](https://doi.org/10.1021/acs.jmedchem.5b00230).
- 10 P. S. Hellwig, T. J. Peglow, F. Penteado, L. Bagnoli, G. Perin and E. J. Lenardão, Recent Advances in the Synthesis of Selenophenes and Their Derivatives, *Molecules*, 2020, **25**, 5907, DOI: [10.3390/molecules25245907](https://doi.org/10.3390/molecules25245907).
- 11 W. Wu, W. Liu, D. Song and L. Yan, Synthetic routes to selenophenes (biologically valuable molecules), *Synth. Commun.*, 2021, **51**, 2924–2943, DOI: [10.1080/00397911.2021.1958229](https://doi.org/10.1080/00397911.2021.1958229).
- 12 R. A. Kjønaas and S. P. Mattingly, Acid-Catalyzed Isomerization of Carvone to Carvacrol, *J. Chem. Educ.*, 2005, **82**, 1813, DOI: [10.1021/ed082p1813](https://doi.org/10.1021/ed082p1813).
- 13 N. W. Tideswell and J. D. McCullough, Selenium Bromides. I. A Spectrophotometric Study of the Dissociation of Selenium Tetrabromide and Selenium Dibromide in Carbon Tetrachloride Solution, *J. Am. Chem. Soc.*, 1956, **78**, 3026–3029, DOI: [10.1021/ja01594a025](https://doi.org/10.1021/ja01594a025).
- 14 M. Lamoureux and J. Milne, Selenium chloride and bromide equilibria in aprotic solvents; a  $^{77}\text{Se}$  NMR study,





- Polyhedron*, 1990, **9**, 589–595, DOI: [10.1016/S0277-5387\(00\)86238-5](#).
- 15 (a) R. G. Parr and W. Yang, *Density Functional Theory of Atoms and Molecules*, Oxford University Press, New York, 1989; (b) Free energy values were obtained at the PBE0-D3/6-311++G(d,p)//PBE0/6-31+G(d,p) level using the Gaussian 09 package. All calculations included solvent effects using the PCM/SMD model. A full account of the computational details and a complete list of references are provided in the ESI.†
  - 16 T. Wirth, G. Fragale and M. Spichly, Mechanistic Course of the Asymmetric Methoxyselenenylation Reaction, *J. Am. Chem. Soc.*, 1998, **120**, 3376–3381, DOI: [10.1021/ja974177d](#).
  - 17 O. E. Edwards and C. Grieco, Displacement at Tertiary Carbon, *Can. J. Chem.*, 1974, **52**, 3561, DOI: [10.1139/v74-531](#).
  - 18 M. Mascal, N. Hafezi and M. D. Toney, 1,4,7-Trimethyloxatriquinane: SN2 Reaction at Tertiary Carbon, *J. Am. Chem. Soc.*, 2010, **132**, 10662–10664, DOI: [10.1021/ja103880c](#).
  - 19 Y.-Q. Zhang, C. Poppel, A. Panfilova, F. Bohle, S. Grimme and A. Gansäuer, SN2 Reactions at Tertiary Carbon Centers in Epoxides, *Angew. Chem., Int. Ed.*, 2017, **56**, 9719–9722, DOI: [10.1002/anie.201702882](#).
  - 20 C. R. Groom, I. J. Bruno, M. P. Lightfoot and S. C. Ward, The Cambridge Structural Database, *Acta Crystallogr., Sect. B: Struct. Sci., Cryst. Eng. Mater.*, 2016, **72**, 171–179, DOI: [10.1107/S2052520616003954](#).
  - 21 F. H. Allen, O. Kennard, D. G. Watson, L. Brammer, A. G. Orpen and R. Taylor, Tables of bond lengths determined by X-ray and neutron diffraction. Part 1. Bond lengths in organic compounds, *J. Chem. Soc., Perkin Trans. 2*, 1987, S1–S19, DOI: [10.1039/P29870000051](#).
  - 22 F. Kumakura, B. Mishra, K. I. Priyadarsini and M. Iwaoka, A Water-Soluble Cyclic Selenide with Enhanced Glutathione Peroxidase-Like Catalytic Activities, *Eur. J. Org. Chem.*, 2010, 440–445, DOI: [10.1002/ejoc.200901114](#).
  - 23 J. P. Telo, Synthesis of (-)-carvone, in *Comprehensive Organic Chemistry Experiments for the Laboratory Classroom*, ed. C. A. M. Afonso, N. R. Candeias, D. P. Simão, A. F. Trindade, J. A. S. Coelho, B. Tan and R. Franzén, The Royal Society of Chemistry, 2016, pp. 244–246.

